Aerosol and Air Quality Research, 12: 911–922, 2012

ISSN: 1680-8584 print / 2071-1409 online
doi: 10.4209/aaqr.2012.01.0018

Vertical Profile and Spatial Distribution of Ozone and Its Precursors at the Inland and Offshore of an Industrial City

Hsieh-Hung Tsai[1], Yu-Fu Liu[1], Chung-Shin Yuan[1*], Wei-Hsiang Chen[1], Yuan-Chung Lin[1], Chung-Hsuang Hung[2], Chitsan Lin[3], Yi-Hsiu Jen[1], Iau-Ren Ie[1], Horng-Yu Yang[4]

[1] *Institute of Environmental Engineering, National Sun Yat-Sen University, Kaohsiung 804, Taiwan*
[2] *Department of Safety, Health and Environmental Engineering, National Kaohsiung First University of Science & Technology, Kaohsiung 811, Taiwan*
[3] *Department of Marine Environmental Engineering, National Kaohsiung Marine University, Kaohsiung 811, Taiwan*
[4] *Department of Civil Engineering, China University of Science and Technology, Taipei 115, Taiwan*

ABSTRACT

This study investigated the ozone formation mechanism and air mass trajectory via simultaneous air quality sampling around the coastal region of urban Kaohsiung. Vertical concentration profiles of O_3 and its precursors (NO_x and VOCs) were sampled and measured at inland and offshore sites during eight intensive sampling periods. The intensive sampling periods were divided into three categories based on meteorological condition: the sea-land breeze period, the northeastern monsoon period, and the mixed period. Vertical profile results showed that the stratification of O_3 was commonly observed at 40 out of 64 sampling sites accounting for 62.5% of the total O_3 measurement. The results obtained from VOCs measurement indicated that the major species of VOCs was acetone, which accounted for 16.25–64.05% of total TVOCs-C_2 in the offshore region, while the major species of VOCs in the inland region was toluene, which accounted for 6.41–43.77 % of total TVOCs-C_2. Backward trajectories showed that air pollutants emitted from land sources could transport to the offshore region, resulting in a high concentration of oversea NO_x and VOCs. Major species of VOCs with high O_3 formation potential were found to be aromatics in the low atmosphere around the coastal region of metro Kaohsiung.

Keywords: Ozone and its precursors; Vertical profile; Stratification phenomenon; Meteorological condition.

INTRODUCTION

Kaohsiung-Pindong air quality zone (KP air quality zone), covering Kaohsiung City and Pindong County, has been officially labeled by Taiwan's Environmental Protection Administration (TEPA) as the worst air quality region (6–8% of poor air quality with PSI > 100) among seven Air Quality Zones (AQZ) in Taiwan (Tsai *et al.*, 2010). Moreover, major ambient air pollutants in metro Kaohsiung are mostly higher than that those at other AQZs in Taiwan (Tsai *et al.*, 2008). Among them, O_3 and PM_{10} are two major air pollutants that are responsible for poor air quality in metro city (Cheng *et al.*, 2010; Chakraborty and Gupta, 2010; Huang *et al.*, 2010; Lee *et al.*, 2010; Reddy *et al.*, 2011; Stone *et al.*, 2011). Previous investigators reported that high O_3 concentration formation had a relationship with nitrogen oxides and hydrocarbon emissions, and under certain weather conditions (eg. high temperature, low wind speed, high radiation, and low humidity), the related photochemical reactions become more vigorous, causing O_3 to accumulate in the low atmosphere (Ball and Bernard, 1978; Comrie and Yarnal, 1992; Han *et al.*, 2011).

Ozone is considered as the principal product of tropospheric photochemical chemistry. High O_3 concentration is a major environmental concern due to its adverse impacts on human health and its key role in the photochemical reaction cycles affecting the formation and fate of its precursors (NO_x and VOCs). In other words, it is of importance to reduce the ambient concentrations of NO_x and VOCs in order to decrease O_3 concentration. There is a non-linear relationship between the concentrations of these two species and the formation concentration of O_3 (Na *et al.*, 2005), and the ratios of [TVOCs-C_2]/[NO_x] in the offshore regions near Kaohsiung are high, indicating that O_3 formation in these regions is NO_x-limited. Thus, NO_x emission must be controlled to prevent the formation of O_3. However, the ratios of [TVOCs-C_2]/[NO_x] in the inland regions are relatively lower, the ratio of some cases were even below 4, showing that O_3 formation is VOCs-limited. Consequently, VOCs emission must be controlled in the

* Corresponding author. Tel.: 886-7-5252000 ext. 4409; Fax: 886-7-5254449
E-mail address: ycsngi@mail.nsysu.edu.tw

inland regions to prevent the formation of O_3. In this work, TVOCs-C_2 is defined as a total of 101 species of volatile organic compounds (TVOCs) with the exception of ethylene, acetylene, and ethane (C_2) species. Generally, C_2 dominated TVOC concentration, which might cause misjudgments for the qualitative analysis of GC/MS spectrum (Jenkin and Clemitshaw, 2000).

Sea-land breezes (SLBs) play an important role in transporting air pollutants to and from urban areas on the coast (Tsai *et al.*, 2008, 2010, 2011). Previous studies have investigated the effects of SLBs on the spatial distribution and transport of ambient air pollutants, particularly for O_3 episodes (Nester 1995; Venkatesan *et al.*, 2002; Evtyugina 2006; Tsai *et al.*, 2008). Many studies indicate that SLBs may transport air pollutants from coastal polluted areas to inland and spread O_3 to an onshore distance of 20–60 km (Kitada and Kitagawa, 1990; Seinfeld and Pandis, 1998; Hastie *et al.*, 1999). Cheng (2002) examined the impact of SLBs on the horizontal distribution of O_3 concentration in the coastal region of Central Taiwan. He concluded that the weak southeastward breeze is the dominant factor affecting the occurrence of O_3 episodes. Moreover, Liu *et al.* (1994) found high O_3 episodes occur at the downwind of sea breeze in Taipei and Kaohsiung.

Previous investigators reported that, in recent decades, towers, tethered balloons, aircraft, and lidar have all been applied to measure vertical profiles (Chen *et al.*, 2002). In this study, the vertical concentration profiles of O_3 and its precursors (NO_x and VOCs) at eight sites were sampled by tethered balloons with unreactive air sampling diaphragm pumps and black tedlar bags. This method has been used to investigate the vertical profile and the tempospatial distribution of ozone and its precursors in the low atmosphere. This study further investigated the ozone formation mechanism and air mass trajectory via simultaneous air quality sampling over the coastal region of metro Kaohsiung. This work presents the vertical distributions of ozone concentrations and its precursors, as measured via tethered balloons and sampling pumps at Kaohsiung City.

EXPERIMENTAL METHODS

Ozone and its precursors were simultaneously sampled both inland and offshore during eight intensive sampling periods on August 16–18 and November 2–4, 2006; January 24–26, March 6–8, and May 2–4, 2007; October 30–November 1, 2008; and March 11–13 and July 15–17, 2009. Sampling of inland O_3 and its precursors was conducted at sixteen sites located in southern Taiwan, including ten Taiwan Air Quality Monitoring Network (TAQMN) sites and six other sites established for this particular study. The six latter sites for intensive sampling were located at National Kaohsiung University (NKU), National Kaohsiung First University of Science & Technology (NKFUST), Zuoying Junior High School (ZYJ), Chisian Junior High School (CSJ), Jhongyun Junior High School (JYJ), and Fooyin College (FYC). At each inland sampling site, a mobile air quality monitoring vehicle with an O_3 analyzer (ML 9812) and a NO_x analyzer (DANI 200A) was used to simultaneously monitor O_3 and NO_x, as shown in Table 1. After sampling, O_3 and NO_x in the tedlar bag were analyzed with on-line instruments immediately, and volatile organic compounds (VOCs) were sampled with a stainless steel canister and further analyzed with a gas chromatography-mass spectrometry (HP 6890N GC/MS) and a thermal-desorption unit (ENTECH 7100A Preconcentrator). A 0.25 mm Chrompack DB-1 60 m-length capillary column was employed for qualitative analysis. Spectrum gases for calibration curves in quantities follow the standard gas of NIEA A715.14B (i.e. US EPA Method TO-15).

Sampling of offshore O_3 and its precursors were conducted at two offshore locations, including Hsiau-Liu-Chiou (HLC), an island approximately 10 km away from the southwestern coast of Kaohsiung City, and a mobile air quality monitoring boat navigated to positions approximately 5–12 km away from the coastline of Kaohsiung City. The locations of inland and offshore sites for sampling O_3 and its precursors around the coastal region of Kaohsiung City are shown in Fig. 1. During each intensive sampling period of 48 h, sampling of O_3 and its precursors were conducted simultaneously at both offshore and inland sites. Offshore O_3 and its precursors were sampled at the top floor on the front deck of the boat to prevent the interferences from the exhaust tail gases of the boat and from oceanic spray. Like the inland sampling, offshore O_3 and its precursors were also measured with O_3 and NO_x analyzers, and VOCs was preserved by stainless steel canister.

During the intensive sampling periods, O_3 and NO_x concentrations were measured over a 48 h period, while VOCs were sampled using two black tedlar bags (SKC, 233–08B) at 3 h intervals. This bag was frequently used for collecting and protecting light-sensitive compounds to avoid the requirement for cumbersome outer containers. In addition, the analytical method for the US EPA Method TO-15 used in this work involves using a high resolution GC/MS (HP, 6890N) at each sampling site. The meteorological data was also monitored over a 48 h period to obtain the hourly average value for the ground level time-intensive sampling data. The vertical profiles of O_3, NO_x, and VOCs were also simultaneously measured in the atmosphere. During the

Table 1. The principles and standard methods of O_3 and NO_x analyzer.

Analyzers	Brands/Models	Principles	Standard Methods
Ozone analyzer	ML 9812	Ultraviolet absorption	[a]NIEA A420.10T
Nitrgen oxides analyzer	DANI 200A	Chemiluminescence	[a]NIEA A417.10T
Gas chromatography-mass spectrometry	HP 6890N	Separates chemical mixtures and identifies the components at a molecular level	[a]NIEA A715.14B

[a]NIEA: National Institute of Environmental Analysis, Taiwan.

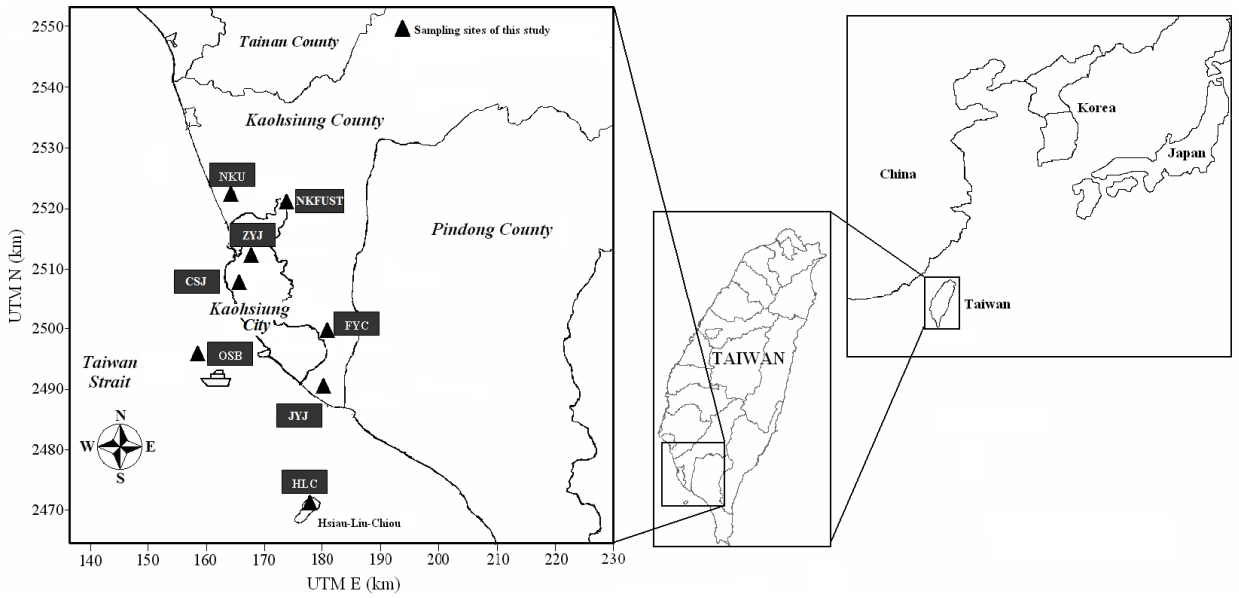

Fig. 1. Location of inland and offshore sampling sites over the coastal region of metro Kaohsiung.

intensive sampling periods, vertical O_3 and NO_x concentration profiles were recorded at 3 h intervals–8:00 am, 11:00 am, 2:00 pm, 5:00 pm, 8:00 pm, 11:00 pm, 2:00 am, and 5:00 am Local Time (LT), starting at 8:00 am. Among them, the first to fifth samples were taken at an altitude of 100 m above ground from 2006 to 2007, while the last three samples were taken at an altitude of 500 m at NKU, NKFUST, FYC, ZYJ, and HLC, respectively. In addition, a mobile air quality monitoring boat collected a total of 34 sampling data sets of O_3 and NO_x at an altitude of 200 m from 2008 to 2009. A total of 16 sampling data sets of VOCs at the altitudes of 0, 100, 300, and 500 m above ground were collected every 6 hours for a 48 h sampling starting at 8:00 am Local Time (LT) at FYC, JYJ, and HLC, respectively.

This study used a tethered balloon technique to acquire the vertical and spatial distributions of O_3 and its precursors at the altitudes of 0 m, 100 m, 200 m, 300 m, and 500 m above ground (Cheng, 2002). The vertical profile measurements of O_3 and its precursors given here were obtained by using a tethered balloon with the attachment of electric winch, ropes, air pumps (SKC 224–PCXR miniature diaphragm pumps for personal or environmental sampling of gases and vapors in air), and tedlar bags, which could reach an altitude up to 500 m. A specially designed lightweight (936 g) air sampling pump with a timer was utilized to inflate two tedlar bags. After sampling, the winch retracted the tether line to retrieve the tedlar bags. The time setting was different depending on the sampling heights. In general, the higher the balloon was raised, the longer the delay time was set before sampling began. For example, the delay times were set as 4, 12 and 20 min, when the sampling points were set at 100, 300, and 500 m above ground, respectively. When the balloon reached its proper height, the timer-controlled sampling pump was automatically turned on and provided a constant flow rate to the tedlar bags for 6 min, and the sampling pump was then automatically shut down and the unit lowered down the tethered balloon by using the electric winch. Two tedlar bags were then removed. Tetherd balloons have been widely applied to suck air samples above ground into two tedlar bags by an air pump (Cheng, 2002; Wu *et al.*, 2010; Sangiorgi *et al.*, 2011). After sampling, one tedlar bag was quickly connected to the air inlet of an air quality monitoring automobile for measuring O_3 and NO_x concentrations, respectively. Measurement of O_3 and NO_x for each bag took approximately 2 min. To minimize sampling artifacts by cross contamination, the pump was equipped with a diaphragm membrane. Another tedlar bag was immediately transferred to a stainless steel canister and then brought back to the laboratory for further analysis of VOCs within one week. Moreover, each tedlar bag was covered with a light-shielding bag to avoid photochemical reactions occurred inside the tedlar bag. The device used for the vertical profile sampling is shown in Fig. 2.

Backward trajectory analysis were simulated with an Air Quality Trajectory Model (version 1.1) developed by Taiwan EPA (Chang *et al.*, 1983). The assimilation method incorporates the Barnes objective method to interpolate spatial values and the variation-kinematical model was adopted to correct the effects of complex terrain and to produce hourly wind field data using 24 ground surface stations spread over southern Taiwan (Barnes 1973; Chang *et al.*, 1983). These included two meteorological stations from the Central Weather Bureau of Taiwan (CWBT) and 22 ambient air quality monitoring stations from TAQMN. By utilizing the hourly wind fields over the ground surface, backward trajectories of air parcels were simulated for 10 h at seven selected air quality monitoring stations. The trajectories were simulated by using the horizontal wind components only, with a segment time resolution of 1 h, and the interpolation was linear in both time and space domain. The initial time of backward trajectory for each monitoring station was determined whenas the maximum hourly O_3 concentrations were observed.

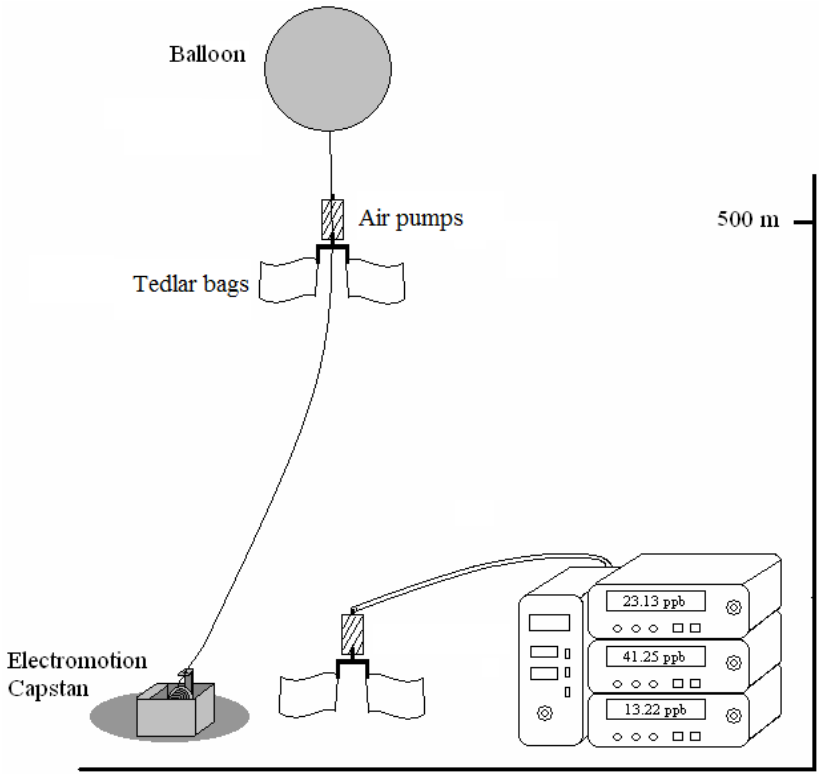

Fig. 2. Illustration of the tethered balloon sampling and analytical instruments in the field.

RESULTS AND DISCUSSION

Meteorological Measurement Data

Taiwan is geologically located in the East Asian subtropical zone, and is significantly influenced by the northeastern monsoon (NEM) blown from late fall to late spring and by the southwestern monsoon blown from summer to mid-fall. A sea breeze is superimposed on these monsoons when meteorological conditions are suitable to produce daytime northwesterly or southwesterly flow. This study collected the meteorological data from ambient air quality monitoring stations operated by TAQMN and CWBT in the KP air quality zone during eight intensive sampling periods from August 2006 to July 2009. Wind speed and wind direction data shown in Table 2 were used to characterize the intensive sampling periods into three categories: the sea-land breeze (SLB) period (the first, fifth, and eighth sampling periods), the northeastern monsoon (NEM) period (the third, fourth, and seventh sampling periods), and the mixed (MIX) period (the second and sixth sampling periods). During the SLB periods, the wind direction changed for at least 90° between daytime (daytime sampling was conducted at 8:00 am, 11:00 am, 2:00 pm, and 5:00 pm) and nighttime (nighttime sampling was conducted at 8:00 pm, 11:00 pm, and 2:00 am, and 5:00 am), and the wind speeds of sea breezes varied much more significantly than those of land breezes. There was an obvious interaction between sea and land breezes, when the wind direction

Table 2. Wind direction, wind speeds, and wind field categories for eight intensive sampling periods.

Sampling Periods	Sampling Time	Wind Direction (Time)	Wind Speeds (m/sec)	Wind Field Categories
#1	Aug. 16–18, 2006	Sea breeze: 300°–350° (10:00–23:00) Land breeze: 330°–60° (23:00–10:00)	1–4 1–4	SLB
#2	Nov. 2–4, 2006	270°–30°, 0°–60°	1–3	MIX
#3	Jan. 24–26, 2007	300°–30°	1–3	NEM
#4	Mar. 6–8, 2007	300°–40°	1–3	NEM
#5	May 2–4, 2007	Sea breeze: 240°–330° (09:00–21:00) Land breeze: 330°–60° (21:00–09:00)	1–5 1–5	SLB
#6	Oct. 30–Nov. 1, 2008,	270°–315°, 0°–90°	1–3	MIX
#7	Mar. 11–13, 2009	300°–60°	1–4	NEM
#8	Jul. 15–17, 2009	Sea breeze: 240°–330° (09:00–23:00) Land breeze: 300°–350° (23:00–09:00)	1–3 1–3	SLB

SLB: sea-land breeze; NEM: northeastern monsoon; MIX: mix wind field.

transformed a land breeze to a sea breeze at 9:00–10:00 am, and a sea breeze to a land breeze at 9:00–11:00 pm, and the wind speed also varied significantly during the interaction periods. During the NEM periods, the prevailing wind blew from the north (300–60°) with the average speeds of 1–4 m/s. During the MIX periods, the wind direction varied significantly from 270° to 90° with the average wind speeds of 1–3 m/s. In addition, previous investigators reported that the sea breeze speed is higher than land breeze speed, since sea regions have less friction than land ones (Ozoe *et al.*, 1983).

Vertical Distribution of O_3 Concentration

The spatial distribution and temporal variation of O_3 concentration were monitored over the coastal region of metro Kaohsiung during the SLB, NEM, and MIX periods. A single modal variation of O_3 was observed over the coastal region. During the SLB periods, O_3 appeared after sunrise and its level at the inland sites was relatively lower than the offshore sites in the early morning. Photochemical reaction forming O_3 in the atmosphere resulted in the highest O_3 concentration mostly at noon at the inland sites. The highest O_3 concentration of approximately 150 ppb at the inland sites was observed on May 2–4, 2007. At nighttime, O_3 and its precursors accumulated in the coastal region had a tendency to transport from the land to the sea due to land breezes, which resulted in relatively higher O_3 concentration at the offshore sites than that at the inland sites. O_3 was formed mainly in the daytime and then accumulated at nighttime. During the MIX periods, field measurement results showed that the highest O_3 concentrations were observed at the inland sites in the daytime and at the offshore sites at nighttime. The highest O_3 concentration of approximately 130 ppb was observed at the inland sites at 14:00 on October 31, 2007. During the NEM periods, O_3 concentrations with an average of 48.54 ppb at the inland sites were mostly higher than those with an average of 32.17 ppb at the offshore sites. On the contrary, high O_3 concentrations observed at inland during the NEM periods were mainly influenced by the northerly winds, which transported O_3 from the northern region to metro Kaohsiung.

Field measurement results also indicated that the variation trend of O_3 concentration at the ground level was similar to that at 100–500 m above the ground, although O_3 concentration at 100 m was higher than that at the ground level over the coastal region. However, no matter in the daytime or at nighttime, the average O_3 concentration at the ground level was at least 3 times higher than that above the ground (100 m) at four sampling sites on March 6–8, 2007. The results implied that O_3 could be formed and accumulated at 100 m over the coastal region. It suggested that the sunshine at 100 m was somehow stronger than that at the ground level, which influenced the lifetime of ozone formation/sink and the time constant of mixing. Additionally, NO_x emitted from high chimney could titrate with O_3 and reduce its concentration above 100 m, resulting in a maximum O_3 concentration at 100 m above ground (Wu *et al.*, 2010). Further investigation on O_3 accumulation showed that O_3 concentration at 500 m was 40.45 ppb at the offshore HLC site during the secondary intensive sampling period. At nighttime, O_3 concentration at the ground level and above the ground was relatively high at the offshore sites. Vertical profiles of O_3 concentration at inland and offshore sites are illustrated in Fig. 3. On October 30, a high O_3 concentration was observed at 2:00 pm at the offshore site HCL. Ozone concentration at 100–500 m was higher than the ground O_3 level, with a core up to 85 ppb at 300–500 m, contributing to serious O_3 episodes at the downwind region of metro Kaohsiung. At nighttime, O_3 concentration tended to decrease at the coastal region due to land breezes. A backward trajectory model was used to determine the transportation routes of O_3 before they arrived at the sampling locations.

Stratification Phenomenon of O_3 and its Precursors (NO_x and VOCs)

In this study, TVOCs-C_2 is defined as a total of 101 species of volatile organic compounds (TVOCs) with the exception of ethylene, acetylene, and ethane (C_2) species. Generally, C_2 dominated TVOCs concentration, which may cause misjudgments for data analysis. In this study, stratification factor was defined as the ratio of the concentrations of air pollutants sampled at 100, 300, and 500 m above ground to those sampled on the ground. The data shown in Table 3 are the mean value of stratification factor in the daytime and at nighttime. The turn-over of TVOC-C_2 concentrations were observed for different altitudes (100, 300, and 500 m above ground) at 19 sampling sites, accounting for 63% of total 30 sampling sites in the daytime. The results showed that the stratification phenomenon occurred frequently at both inland and offshore sites. At nighttime, the turn-over of TVOC-C_2 concentrations for different altitudes were measured at 15 sampling sites, accounting for 50% of total 30 sampling sites, and the results showed that the stratification phenomenon occurred mainly at inland sites (a total of 10 sites). The turn-over of NO_x concentrations at the altitudes of 100, 300, and 500 m above ground had 17 sampling sites, accounting for 53% of total 32 sampling sites of the daytime, and the stratification phenomenon occurred at inland and offshore sites; at nighttime, the turn-over of NO_x concentrations at different altitudes were measured at 13 sampling sites, accounting for 41% of total 32 sampling sites, and the stratification phenomenon occurred mainly at offshore sites (a total of 11 sites). Overall, during the eight intensive sampling periods, the stratification of O_3 concentration occurred at 40 out of 64 sampling sites, in which its precursors (NO_x and VOCs) demonstrated their stratification phenomenon at 30 sampling sites, accounting for 75% of total O_3 stratification. This phenomenon is mainly attributed to the facts that air pollutants can be accumulated in the mixing layer over the coastal region (Lin *et al.*, 2007).

Major Species of Volatile Organic Compounds for Different Wind Field Categories

In this study, 46 species of TVOCs-C_2 were divided into four categories: alkanes, alkenes, aromatics, and carbonyls, as illustrated in Fig. 4. During the SLB periods (Fig. 4(a)),

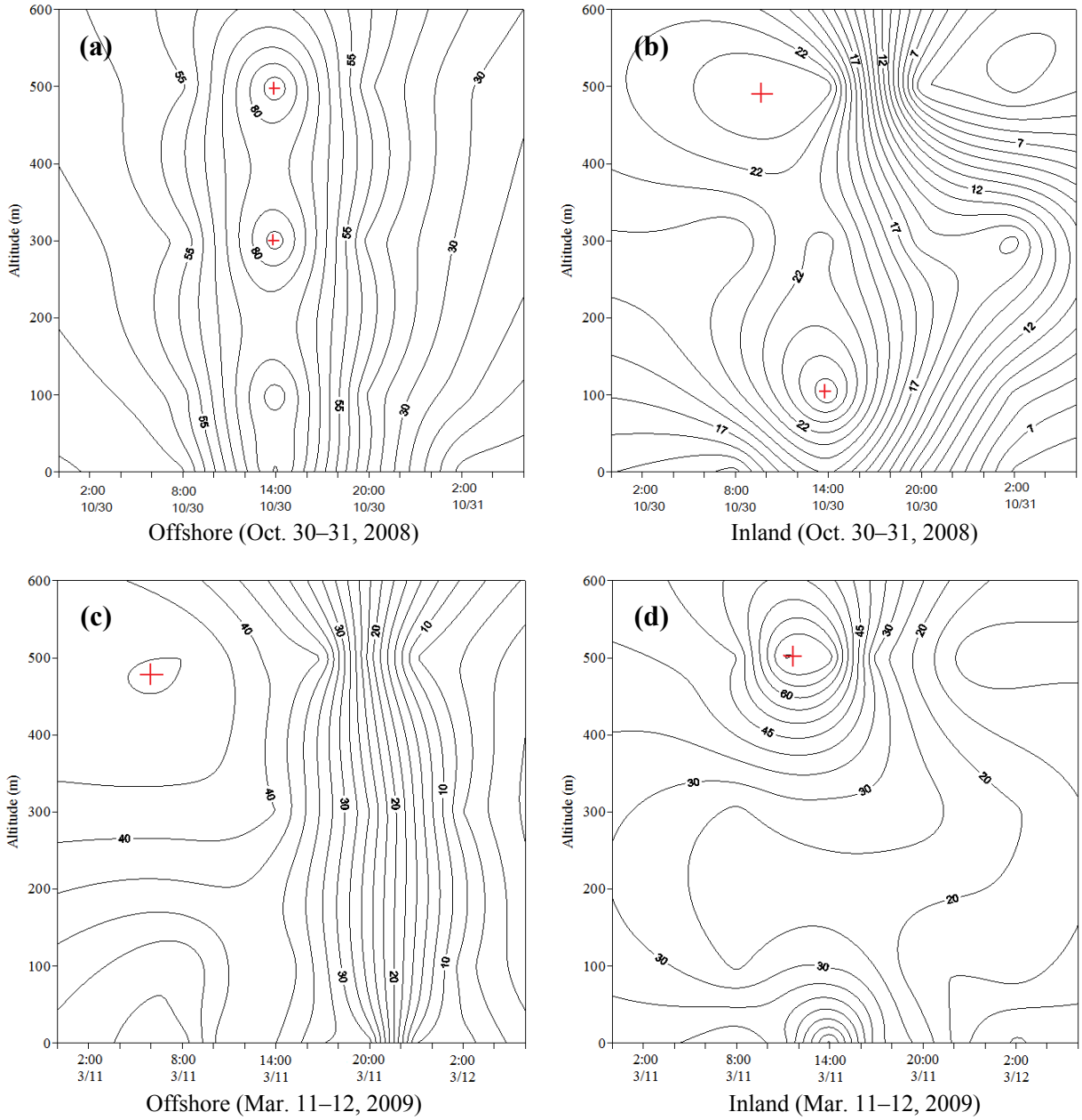

Fig. 3. Vertical distribution of O_3 concentration at inland and offshore sites over the coastal region of metro Kaohsiung in the unit of ppb.

the major species of TVOCs-C_2 were aromatics. The concentrations of aromatics in the inland region in the daytime and at nighttime were 7.99–22.98 μg/m^3 and 7.08–61.50 μg/m^3, respectively, and those in the offshore region were 28.55-72.47μg/m^3 and 25.20–39.25 μg/m^3, respectively. At nighttime, the proportion of aromatics increased in TVOCs-C_2 in the offshore region, with an average concentration accounted for 139–246% of the daytime level, indicating that the effect of industrial pollution became significant as land breezes blew at nighttime, and the major species of TVOCs-C_2 were aromatics which accounted for 29.79–51.27% of TVOCs-C_2 in the inland region. During the NEM periods (Fig. 4 (b)), the concentrations of carbonyls in the inland region in the daytime and at nighttime were 14.26–74.87 μg/m^3 and 20.37–43.37 μg/m^3, respectively, and those in the offshore region were 20.74–40.14 μg/m^3 and 22.14–51.72 μg/m^3, respectively. The major species of TVOCs-C_2 were alkanes and carbonyls which accounted for 28.00–56.15% and 20.59–55.64% of TVOCs-C_2 in the offshore region, respectively; while the major species of TVOCs-C_2 were alkanes, aromatics, and carbonyls, which accounted for 71.25–95.61% of TVOCs-C_2 in the inland region. The TVOCs-C_2 ratio showed no significant change from ground level to a high altitude. During the MIX periods (Fig. 4(c)), the concentrations of alkenes in the inland region in the daytime and at nighttime were 2.62–4.81 μg/m^3 and 2.97–11.51 μg/m^3, respectively, and those in the offshore region were 3.97–5.30 μg/m^3 and 2.52–3.91

Table 3. Means of stratification of O_3 and its precursors (NO_x and VOCs) at inland and offshore sites during eight intensive sampling periods.

[a] Sampling Periods	HLC Site			OSB Site			FYC Site			[b] CSJ or JYJ Site		
Daytime	O_3	NO_x	VOCs	O_3	NO_x	VOCs	O_3	NO_x	VOCs	O_3	NO_x	VOCs
#1 (n = 16)	1.64	1.14	1.75	1.18	1.15	8.33	1.22	1.32	< 1	1.04	1.01	1.52
#2 (n = 16)	1.18	1.47	2.04	< 1	< 1	< 1	1.35	< 1	< 1	< 1	< 1	< 1
#3 (n = 16)	< 1	1.03	—	1.89	1.06	3.57	< 1	1.08	2.63	1.61	< 1	2.22
#4 (n = 16)	1.11	< 1	—	1.64	1.03	1.47	2.00	< 1	1.15	3.13	1.02	1.89
#5 (n = 16)	1.08	1.11	< 1	< 1	< 1	1.61	1.39	1.05	< 1	< 1	< 1	1.69
#6 (n = 16)	1.20	1.02	< 1	< 1	1.37	< 1	< 1	1.16	< 1	< 1	< 1	1.08
#7 (n = 16)	< 1	< 1	3.33	1.04	1.28	< 1	1.05	< 1	< 1	< 1	< 1	< 1
#8 (n = 16)	1.33	< 1	1.89	1.02	< 1	< 1	< 1	< 1	< 1	< 1	1.15	1.08
Nighttime	O_3	NO_x	VOCs	O_3	NO_x	VOCs	O_3	NO_x	VOCs	O_3	NO_x	VOCs
#1 (n = 16)	1.25	1.12	2.70	1.54	1.30	> 100	1.54	< 1	< 1	< 1	< 1	< 1
#2 (n = 16)	1.69	1.18	1.14	1.41	< 1	< 1	2.86	< 1	1.19	1.22	< 1	1.49
#3 (n = 16)	1.79	1.03	—	2.78	< 1	4.00	1.12	< 1	4.55	2.70	< 1	2.04
#4 (n = 16)	1.96	< 1	—	1.82	< 1	1.04	2.33	< 1	1.64	4.00	< 1	1.39
#5 (n = 16)	< 1	1.35	< 1	< 1	1.18	< 1	2.13	< 1	< 1	1.11	< 1	< 1
#6 (n = 16)	1.52	1.16	< 1	1.08	1.45	< 1	< 1	1.28	1.82	< 1	1.14	< 1
#7 (n = 16)	< 1	1.28	< 1	< 1	1.01	1.14	1.49	< 1	< 1	< 1	< 1	1.02
#8 (n = 16)	1.45	< 1	2.38	< 1	1.23	< 1	< 1	< 1	< 1	< 1	< 1	< 1

1. [a] Sampling periods #1–#8 are shown in Table 2.
2. [b] CSJ site was chosen for sampling periods #1–#5 and JYJ site was chosen for sampling periods #6–#8.
3. Stratification factor is defined as the ratio of the concentrations of air pollutants sampled at 100, 300, 500 m above ground to those sampled on ground level. The data shown in Table 3 are the mean value of stratification factor in the daytime and at nighttime.
4. "—" means no sample available; "< 1" means no stratification; "> 1" means stratification occurrence.
5. Daytime sampling was conducted at 8:00 am, 11:00 am, 2:00 pm, while 5:00 pm, while nighttime sampling was conducted at 8:00 pm, 11:00 pm, 2:00 am, and 5:00 am.

μg/m^3, respectively. A significant vertical variation of TVOCs-C_2 ratio was observed from ground level to a high altitude in the offshore region. The major species of TVOCs-C2 were alkanes and carbonyls, which accounted for 69.83% and 74.01% of TVOCs-C_2 at ground level in the daytime and at nighttime, respectively. The major species of TVOCs-C_2 were aromatics, which accounted for 49.26% and 35.71% of TVOCs-C_2 at 100–200 m above ground in the daytime and at nighttime, respectively. The major species of TVOCs-C_2 were carbonyls, which accounted for 65.74% and 40.33% of TVOCs-C_2 at 300–500 m above ground in the daytime and at nighttime, respectively. The major species of TVOCs-C_2 were alkanes, aromatics, and carbonyls in the inland region. In general, for petrochemical processing and storage tank operations, the major species of TVOCs-C_2 are alkanes, alkenes, and aromatics, while of the major species of TVOCs-C_2 for mobile sources are alkanes and carbonyls. At the offshore region, boat exhaust is the major VOC emission source (Morikawa *et al.*, 1998). In addition, boats coated with painting can emit VOCs to the air (Malherbe *et al.*, 2007). It concluded that TVOCs-C_2 were mainly emitted from industrial sources and automobiles at the inland region, while boat exhaust and painting were the major sources for TVOCs-C_2 at the offshore region.

Analysis of Air Mass Aging

Previous investigators reported on the transmission processes of VOCs at offshore and inland regions in order to determine O_3 episodes derived from VOCs and NO_x sources (Hsieh and Tsai, 2003; Wang *et al.*, 2008). This study used the life cycles of VOCs species to estimate air mass aging and photochemical reactivity. Air mass aging analysis was conducted by using the m,p-xylene/ethylbenzene (m,p-X/E) ratio. In general, the air mass is fresher as the m,p-X/E ratio is larger (Hsieh and Tsai, 2003; Wang *et al.*, 2008). According to the photochemical reactivities, the reaction rate of m,p-xylene was faster, while that of ethylbenzene was slower.

Table 4 lists the m,p-X/E ratio for three wind field categories. During the SLB periods, the sampling altitudes were divided into 0–100 m, 100–200 m, and 300–500 m above ground, and the m,p-X/E ratios in the offshore region were 2.12 ± 0.32, 1.73 ± 0.37, and 1.64 ± 0.21, respectively, while the m,p-X/E ratios in the inland region were 3.52 ± 0.14, 3.64 ± 0.11, and 3.33 ± 0.32, respectively. The results showed that the m,p-X/E ratios in the offshore region were lower than those in the inland region, indicating that the air mass in the offshore region was older than that in the inland region. Moreover, as the altitude reached 300–500 m, the air mass showed an aging trend. During the NEM periods, the m,p-X/E ratios in the offshore region were 2.05 ± 0.11, 2.33 ± 0.52, and 1.82 ± 0.17, respectively. Compared to two

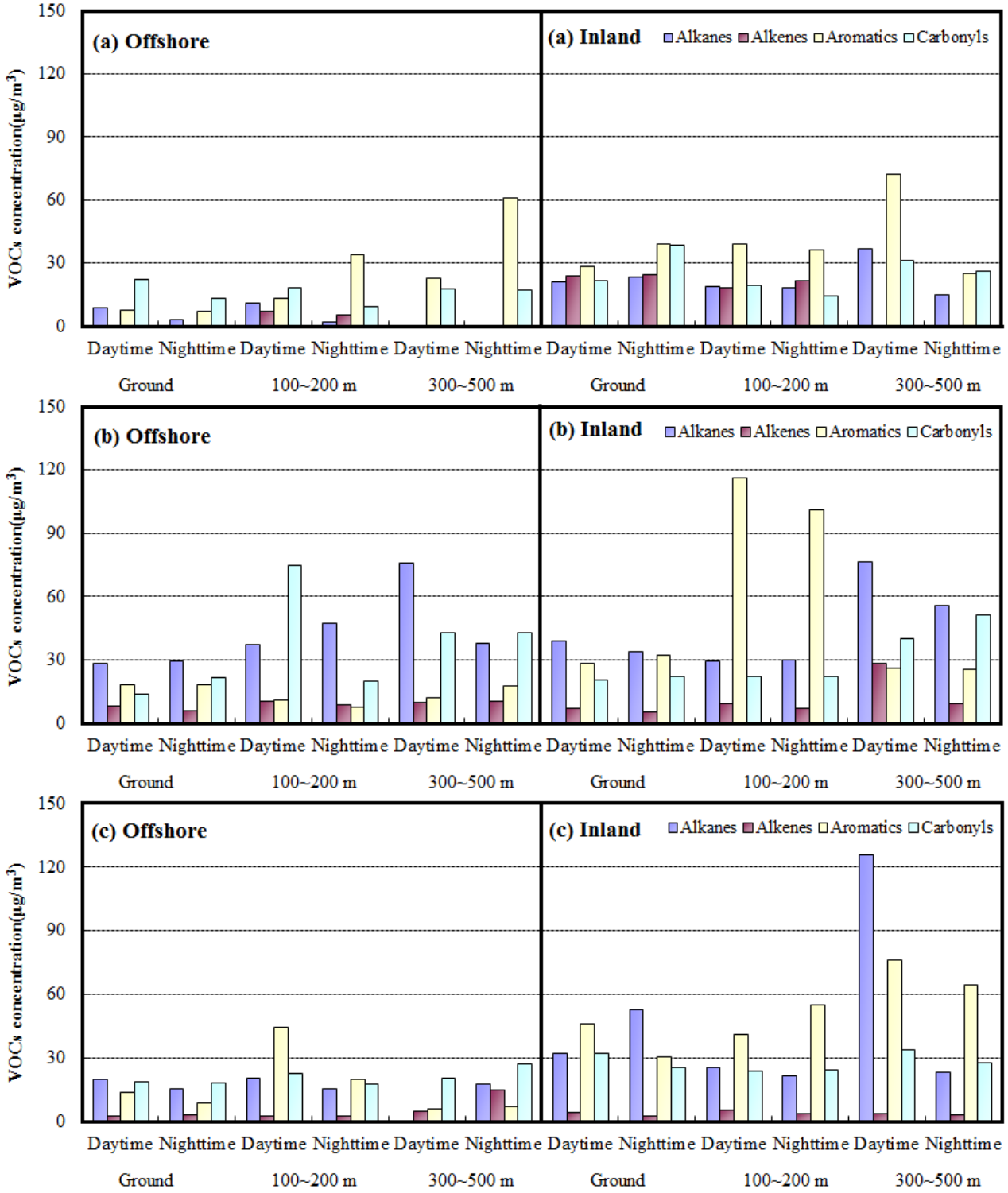

Fig. 4. TVOC-C_2 composition ratio of offshore and inland regions in three wind field categories (a) the SLB periods, (b) the NEM periods, and (c) the MIX periods.

other periods, the m,p-X/E ratios at different heights during the NEM period did not vary much probably due to relatively stable atmosphere. In the inland region, the m,p-X/E ratios were 3.55 ± 0.25, 3.22 ± 0.18, and 3.43 ± 0.26, respectively, and thus the m,p-X/E ratios did not vary much. While the altitude reached 300–500 m, the air mass showed an aging trend in the offshore region. The air mass in the offshore region was generally older than that in the inland region due to the transport of air from the land to the sea, similar to the SLB periods. During the MIX periods, the m,p-X/E ratios in the offshore region were 3.43 ± 0.26, 2.73 ± 0.15, and 2.44 ± 0.33, respectively. In the inland region, the

Table 4. The concentration ratio of m,p-Xylene and Ethylene (m,p-X/E ratio) at different sampling altitudes for three wind field categories.

Wind Field Categories	Sampling Altitudes	m,p-X/E Ratios	
		Offshore	Inland
SLB periods	0–100 m	2.12 ± 0.22	3.52 ± 0.14
	100–300 m	1.73 ± 0.37	3.64 ± 0.11
	300–500 m	1.64 ± 0.21	3.33 ± 0.32
NEM periods	0–100 m	2.05 ± 0.11	3.55 ± 0.25
	100–300 m	2.33 ± 0.52	3.22 ± 0.18
	300–500 m	1.82 ± 0.17	3.43 ± 0.26
MIX periods	0–100 m	3.43 ± 0.26	4.24 ± 0.14
	100–300 m	2.73 ± 0.15	3.63 ± 0.24
	300–500 m	2.44 ± 0.33	3.57 ± 0.32

m,p-X/E ratio is defined as the concentration ratio of m,p-xylene to ethylene.

m,p-X/E ratios were 4.24 ± 0.14, 3.63 ± 0.24, and 3.57 ± 0.32, respectively. The results showed that, as the altitude reached 300–500 m, the air mass became older due to the emissions of VOCs from the ground. In the offshore region, the m,p-X/E ratios during the MIX periods were higher than those during the SLB and NEM periods, showing that the air mass was fresher. Since the atmosphere was unstable, the air mass transportation processes was less polluted in the inland and offshore regions over the coastal region of metro Kaohsiung, resulting from the accumulation of local industrial emission and boat exhausts.

The [TVOCs-C_2]/[NO_x] ratios at different sampling heights for three wind field categories are shown in Table 5. In this study, the [TVOCs-C_2]/[NO_x] ratio influenced the ground and upper levels of O_3 formed by the photochemical reactions between NO_x and VOCs (Blanchard and Fairley, 2001). The [TVOCs-C_2]/[NO_x] ratio at offshore were higher than 8, or even higher than 15. It was showed more based on NO_x-limited, thus reducing O_3 for the generation must be controlled of NO_x reduction. However, the [TVOCs-C_2]/[NO_x] ratio at inland were lower than 8, or even lower than 4, showing that O_3 was VOCs-limited, which addressed the reduction of VOCs concentration, could effectively reduce O_3 concentration. Previous study reported that O_3 formation is mostly VOCs-limited in the vicinity of emission sources, while O_3 formation is mostly NO_x-limited for other places. It is attributed to the fact that the photochemical reaction of NO_x has relatively short life cycle (3 to 6 h) and VOCs in the photochemical reaction cycle need 24 h or more. As a result, the [VOCs]/[NO_x] ratio would be larger. The results suggested that air mass at the altitude of 300–500 m in the offshore region were NO_x-limited during the NEM and MIX periods. High-altitude was mainly affected by long-range transport air mass blown from the central and northern parts of Taiwan due to northeastern monsoon. For other two periods, ground to the altitude O_3 was generated by the impact of both VOCs and NO_x. The results showed that the offshore sites were also influenced by the emissions from inland sources. During the NEM periods, the O_3 formed in the inland region was VOCs-limited, showing that local emission sources were superior to long-range transportation.

Table 5. The [TVOCs-C_2]/[NO_x] ratio at different sampling altitudes for three wind field categories.

Wind Field Categories	Sampling Altitudes	[TVOCs-C_2]/[NO_x]	
		Offshore	Inland
SLB periods	0–100 m	8.12 ± 0.21	6.92 ± 0.12
	100–300 m	8.41 ± 0.11	8.58 ± 0.11
	300–500 m	9.43 ± 0.17	6.14 ± 0.24
NEM periods	0–100 m	6.81 ± 0.36	3.73 ± 0.18
	100–300 m	9.32 ± 0.25	6.41 ± 0.22
	300–500 m	15.05 ± 0.44	8.64 ± 0.15
MIX periods	0–100 m	6.62 ± 0.32	8.15 ± 0.12
	100–300 m	5.97 ± 0.14	6.61 ± 0.13
	300–500 m	16.85 ± 0.47	9.36 ± 0.25

Backward Trajectory Analysis

A backward trajectory model was used to determine the transportation routes of O_3 before it arrived at the monitoring locations. Backward trajectory modeling involves tracing the transportation of air parcels through the meteorological field. Prior to modeling, the meteorological data (mainly wind velocity and wind direction) for the transport of air parcels was gathered from the Taiwan Environmental Protection Administration (TEPA) and Taiwan Central Weather Bureau (TCWB). The backward trajectories of air parcels transported toward the inland air quality monitoring sites around the coastal region of southern Taiwan during the sampling periods are illustrated in Fig. 5.

During the SLB periods (August 16–18, 2006, May 2–4, 2007, and July 15–17, 2009) (see Figs. 5(a)–(c)), sea breezes blown in the early morning could transport the offshore O_3 back to the inland region in southern Taiwan, which resulted in relatively high O_3 concentrations at the inland sites in the afternoon. During the NEM periods (January 24–26, March 6–8, 2007, and March 11–13, 2009) (see Figs. 5(d)–(f)), O_3 was brought to metro Kaohsiung mainly by northerly winds which transported air mass originating from the northern regions (i.e., Chiayi and Tainan Counties). During the MIX periods (November 6–8, 2006 and October 30–November 1, 2009) (Figs. 5(g)–(h)), the wind field was dominated by the northeastern monsoons, and this likely inhibited the influences of sea-land breezes.

In addition to using the m,p-X/E ratio, the analysis of air mass aging in the backward trajectory analysis also showed air pollution transport from the north caused TVOCs-C_2 concentrations to be higher and the age of air mass to be older in the offshore region during the NEM periods. During the SLB periods, the fresh air mass transport from the offshore to the inland regions by sea breezes in the morning caused TVOCs-C_2 concentrations to be lower in the inland region over the coastal region of metro Kaohsiung.

CONCLUSIONS

This study investigated ozone formation mechanisms and air mass trajectories via simultaneous air quality sampling over the coastal region of metro Kaohsiung. This study examined eight sampling periods, and found that the stratification of O_3 concentration appeared to be 40 out of

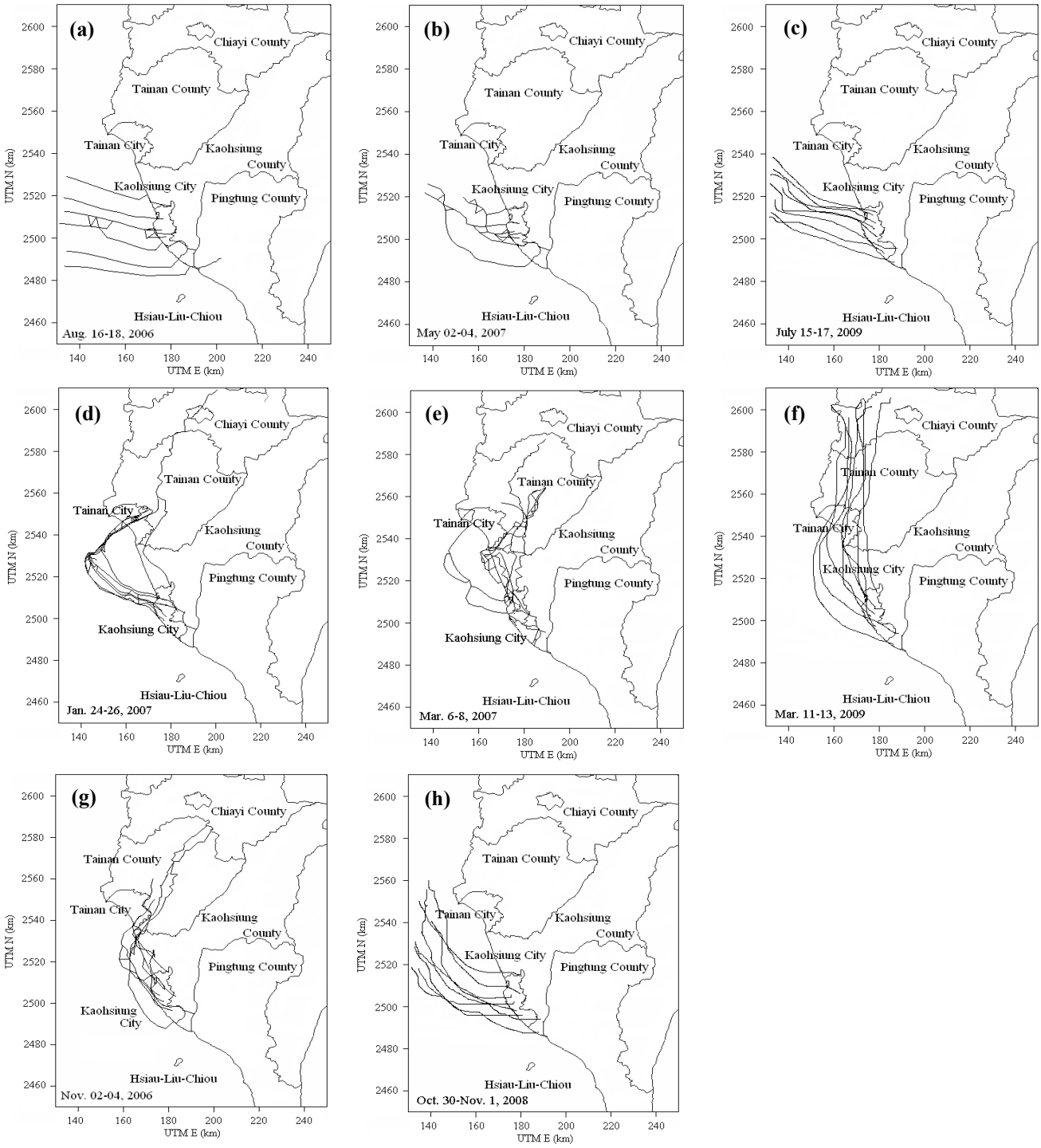

Fig. 5. Backward trajectories of air parcels transported toward the inland sites over the coastal region of southern Taiwan during the SLB periods (a)–(c), the NEM periods (d)–(f), and the MIX periods (g)–(h).

64 sampling sites, in which its precursors demonstrated stratification at 30 sampling sites, accounting for 75% of total O_3 stratification. At nighttime, aromatics dominated TVOCs-C_2 in the offshore region, with an average concentration of 139–246% at the daytime, indicating that when a land breeze was blowing at nighttime, the effect of industrial pollution became more important. The major species of TVOCs-C_2 were aromatics, which accounted for 29.79–51.27% of TVOCs-C_2 in the inland region. The TVOCs-C_2 were mainly emitted from industrial sources and automobiles in the inland region, while boat exhaust and painting were the major sources of TVOCs-C_2 in the offshore region. The analysis of air mass aging showed that air mass in the offshore region was generally older than in the inland region, and the ground air mass was fresher than that at 300–500 m above ground, due to pollution from

emissions sources at the ground level. In the offshore region, the m,p-X/E ratios in the MIX periods were higher than those in the SLB and NEM periods, showing that the air mass was fresher. Due to unstable atmosphere, the air mass transmission processes was less clear in the inland and offshore regions in metro Kaohsiung, and was also affected by local boat exhausts. Backward trajectory analysis further showed that air pollutants transported from the north caused higher TVOCs-C_2 concentrations and the air mass became older in the offshore region during the NEM periods. During the SLB periods, fresh air mass transported from the offshore region to the inland region by sea breezes in the morning caused lower TVOCs-C_2 concentrations in the inland region.

REFERENCES

Ball, D.J. and Bernard, R.E. (1978). An Analysis of Photochemical Pollution Incidents in the Greater London Area with Particular Reference to the Summer of 1976. *Atmos. Environ*. 12: 1391–1401.

Barnes, S.L. (1973). *Mesoscale Objective Map Analysis Using Weighted Time Series Observations*, National Oceanic and Atmospheric Administration, Washington, DC.

Blanchard, C.L. and Fairey, D. (2001). Spatial Mapping of VOC and NO_x-limitation of Ozone Formation in Central California. *Atmos. Environ*. 35: 3861–3873.

Chakraborty, A. and Gupta, T. (2010). Chemical Characterization and Source Apportionment of Submicron (PM_1) Aerosol in Kanpur Region, India. *Aerosol Air Qual. Res*. 10: 433–445.

Chang, L.F.W., Hwang, R.R. and Lin, S.C. (1983). A Variation-Kinematic Model for Flow over Complex Terrain. Annual Report of Institute of Physics. *Acad. Sinica, Taiwan*. 13: 89–102.

Chen, C.L., Tsuang, B.J., Tu, C.Y., Cheng, W.L. and Lin, M.D. (2002) Wintertime Vertical Profiles of Air Pollutants over a Suburban Area in Central Taiwan. *Atmos. Environ.* 36: 2049–2059.

Cheng, W.L. (2002). Ozone Distribution in Coastal Central Taiwan Under Sea-breeze Condition. *Atmos. Environ.* 36: 3445–3459.

Cheng, Y.H. and Lin, Y.L. (2010). Measurement of Particle Mass Concentrations and Size Distributions in an Underground Station. *Aerosol Air Qual. Res*. 10: 22–29.

Comrie, A.C. and Yarnal, B. (1992). Relationships between Synoptic-scale Atmospheric Circulation and Ozone Concentrations in Metropolitan Pittsburgh, Pennsylvania. *Atmos. Environ.* 26: 301–312.

Evtyugina, M.G., Nunes, T., Pio, C. and Costa, C.S. (2006). Photochemical Pollution under Sea Breeze Conditions, during Summer, at the Portuguese West Coast. *Atmos. Environ.* 40: 6277–6293.

Han, S., Bian, H., Feng, Y., Liu, A., Li, X., Zeng, F. and Zhang, X. (2011). Analysis of the Relationship between O_3, NO and NO_2 in Tianjin, China. *Aerosol Air Qual. Res.* 11: 128–139.

Hastie, D.R., Narayan, J., Schiller, C., Niki, H., Shepson, P.B., Sills, D.M.L., Taylor, P.A., Moroz, W.J., Druummond, J.W., Reid, N., Taylor, R., Roussel, P.B. and Melo, O.T. (1999). Observational Evidence for the Impact of the Lake Breeze Circulation on Ozone Concentration in Southern Ontario. *Atmos. Environ.* 33: 323–335.

Hsieh, C.C. and Tsai, J.H. (2003). VOC Concentration Characteristics in Southern Taiwan. *Chemosphere* 50: 545–556.

Huang, L., Wang, K., Yuan, C.S., and Wang, G. (2010). Study on the Seasonal Variation and Source Apportionment of PM_{10} in Harbin, China. *Aerosol Air Qual. Res.* 10: 86–93.

Jenkin, M.E. and Clemitshaw, K.C. (2000). Ozone and other Secondary Photochemical Pollutants Chemical Processes Governing their Formation in the Planetary Boundary Layer. *Atmos. Environ.* 34: 2499–2527.

Kitada, T. and Kitagawa, E. (1990). Numerical Analysis of the Role of Sea Breeze Front on Air Quality in Coastal and Inland Polluted Areas. *Atmos. Environ.* 24: 1545–1559.

Lee, S.B., Bae, G.N., Lee, Y.M., Moon, K.C. and Choi, M. (2010). Correlation between Light Intensity and Ozone Formation for Photochemical Smog in Urban Air of Seoul. *Aerosol Air Qual. Res.* 10: 540–549.

Lin, C.Y., Wang, Z., Chou, C.C.K. and Liu, S.C. (2007). A Numerical Study of an Autumn High Ozone Episode over Southwestern Taiwan. *Atmos. Environ.* 41: 3684–3701.

Liu C.M., Huang, C.Y., Shieh, S.L. and Wu, C.C. (1994) Important Meteorological Parameters for Ozone Episodes Experienced in the Taipei Basin. *Atmos. Environ.* 28: 159–173.

Malherbe, L. and Mandin, C. (2007). VOC Emissions during Outdoor Ship Painting and Health-risk Assessment. *Atmos. Environ.* 41: 6322–6330.

Morikawa, T., Wakamatsu, S., Tanaka, M., Uno, I., Kamiura, T. and Maeda, T. (1998). C2-C5 Hydrocarbon Concentrations in Central Osaka. *Atmos. Environ.* 32: 2007–2016.

Na, K., Moon, K.C. and Kim, Y.P. (2005). Source Contribution to Aromatic VOC Concentration and Ozone Formation Potential in the Atmosphere of Seoul. *Atmos. Environ.* 39: 5517–5524.

Nester, K. (1995). Influence of Sea Breeze Flows on Air Pollution over the Attica Peninsula. *Atmos. Environ.* 29: 3655–3670.

Ozoe, H., Shibata, T. and Sayama, H. (1983). Characteristics of Air Pollution in the Presence of Land and Sea Breeze: A Numerical Simulation. *Atmos. Environ.* 17: 35–42.

Reddy, B.S.K., Reddy, L.S.S., Cao J.J., Kumar, K.R., Balakrishnaiah. G., Gopal, K.R., Reddy, R.R., Narasimhulu, K., Lal, S. and Ahammed, Y.N. (2011). Simultaneous Measurements of Surface Ozone at Two Sites over the Southern Asia: A Comparative Study. *Aerosol Air Qual. Res.* 11: 895–902.

Sangiorgi, G., Ferrero, L., Perrone, M.G., Bolzacchini, E., Duane, M., and Larsen B.R. (2011). Vertical Distribution of Hydrocarbons in the Low Troposphere below and above the Mixing Height: Tethered Balloon Measurements in

Milan, Italy. *Environ. Pollut.* 159: 3545–3552.

Seinfeld, J.H. and Pandis, S.N. (1998). *Atmospheric Chemistry and Physics,* New York: John Wiley & Sons.

Stone, E.A., Yoon, S.C. and Schauer, J.J. (2011). Chemical Characterization of Fine and Coarse Particles in Gosan, Korea during Springtime Dust Events. *Aerosol Air Qual. Res.* 11: 31–43.

Tsai, H.H., Ti T.H., Yuan, C.S., Hung, C.H., and Lin, C. (2008). Effects of Sea-land Breezes on the Spatial and Temporal Distribution of Gaseous Air Pollutants at the Coastal Region of Southern Taiwan. *J. Environ. Eng. Manage.* 18: 387–396.

Tsai, H.H., Yuan, C.S., Huang, C.H. and Lin, Y.C. (2010). Comparing Physicochemical Properties of Ambient Particulate Matter of Hot Spots in a Highly Polluted Air Quality Zone. *Aerosol Air Qual. Res.* 10: 331–344.

Tsai, H.H., Yuan, C.S., Hung, C.H., Lin, C. and Lin, Y.C. (2011). Influence of Sea-land Breezes on the Tempospatial Distribution of Atmospheric Aerosols over Coastal Region. *J. Air Waste Manage. Assoc.* 6: 358–376.

Tsai, H.H., Yuan, C.S., Huang, C.H. and Lin, C. (2011). Physicochemical Properties of $PM_{2.5}$ and $PM_{2.5–10}$ at Inland and Offshore Sites over southeastern Coastal Region of Taiwan Strait. *Aerosol Air Qual. Res.* 11: 664–678.

Venkatesan, R., Mathiyarasu, R. and Somayaji, K.M. (2002). A Study of Atmospheric Dispersion of Radionucleides at a Coastal Site Using a Modified Gaussian Model and a Meso-scale Sea Breeze Model. *Atmos. Environ.* 36: 2933–2942.

Wang, J.L., Wang, C.H., Lai, C.H., Chang, C.C., Liu, Y., Zhang, Y., Liu, S. and Shao, M. (2008). Characterization of Ozone Precursors in the Pearl River Delta by Time Series Observation of Non-methane Hydrocarbons. *Atmos. Environ*. 42: 6233–6246.

Wu, Y.L., Lin, C.H., Lai, C.H., Lai, H.C. and Young, C.Y. (2010). Effects of Local Circulations, Turbulent Internal Boundary Layers, and Elevated Industrial Plumes on Coastal Ozone Pollution in the Downwind Kaohsiung Urban-industrial Complex. *Terr. Atmos. Ocean. Sci.* 21: 343–357.

Received for review, January 22, 2012
Accepted, March 22, 2012